J|A|C|S
COMMUNICATIONS

Published on Web 10/19/2005

Millimeter Scale Alignment of Magnetic Nanoparticle Functionalized Microtubules in Magnetic Fields

Mark Platt,[†] Gayatri Muthukrishnan,[‡] William O. Hancock,*[,‡] and Mary Elizabeth Williams*[,†]

Departments of Chemistry and Bioengineering, The Pennsylvania State University, University Park, Pennsylvania 16802

Received August 24, 2005; E-mail: mbw@chem.psu.edu; wohbio@engr.psu.edu

Biology controls the movement and assembly of structures on all length scales with relative ease; within eukaryotic cells, this task is carried out with microtubules and kinesin motor proteins. Conventional kinesin contains two protein subunits that bind to microtubules, hydrolyze ATP, and together function as a processive, double-headed motor. Kinesin motors travel unidirectionally on the 25 nm diameter cylindrical microtubules, transporting cargo up to a meter in biological systems.[1] Harnessing the unique properties of this motor/track pair has recently become of interest for shuttling microtubules laden with cargo across motor-modified surfaces[2] or conversely by adhering microtubules to a surface while motors with attached cargo "walk" along the tubules.[3] A substantial challenge for their use in hybrid biological devices is to develop the ability to produce microtubule tracks with long-range order, which would enable the control of the transport direction of the cargo-laden motors and potentially enable the assembly of complex nanostructures. To date, a degree of microtubule alignment and orientation has been achieved by the use of complex lithographic techniques,[4] by viscous forces,[5] or by strong magnetic or electric fields applied during tubule polymerization.[6] In this communication, we report the first instance of microtubule functionalization with cobalt ferrite nanoparticles ($CoFe_2O_4$) and the facile use of an externally applied magnetic field to control their placement and orientation on surfaces. This technique allows the microtubules to be aligned in a coparallel manner over unprecedented *millimeter* distances in patterns that follow the shape of the magnetic field lines while retaining their motility.

$CoFe_2O_4$ nanoparticles (14 ± 4 nm diameter) were synthesized via high-temperature reduction and continuous seeding experiments in hexane[7] and transferred into aqueous buffer solutions using a technique previously used for semiconductor nanocrystals.[8] The resulting particles contain a biotin-terminated ligand shell for subsequent attachment via selective neutravidin binding. Microtubules were prepared by copolymerization of biotin- (BTU) and rhodamine-labeled (RTU) tubulin following standard methods,[4] which allowed formation of fluorescently labeled microtubules with a tunable quantity of bound biotin based on the relative ratio of BTU and RTU. Three separate microtubule samples were prepared with 0, 37, or 85% BTU content and stabilized using 10 μM taxol. The microtubules were functionalized with $CoFe_2O_4$ particles by incubation with 0.5 mg/mL of neutravidin (5 min), followed by 3 mg/mL of the biotin-functionalized $CoFe_2O_4$ particles (3 min), and diluted with standard buffer solution (Supporting Information).

A flow cell was constructed by affixing a glass slide to a cover slip with double-sided tape (volume ~ 20 μL); the internal surfaces of the cell were sequentially exposed to buffer solutions containing 5 mg/mL of casein (5 min) and, in some cases, 6.6 μg/mL of hexaHis-tagged *Drosophila melanogaster* kinesin[9] (5 min). The solution containing the magnetic particle functionalized microtubules was then injected into the flow cell. A schematic of the resulting microtubule assembly, magnetic particle-conjugated microtubules bound to kinesin motors on the glass surface, is shown in Figure 1A. To test the effectiveness of controlling and aligning the magnetic particle-modified microtubules, this cell was placed on top of a NdFeB permanent magnet for 3−10 min and visualized using fluorescence microscopy (Figure 1B).

When a casein-passivated surface (in the absence of kinesin motors) was used, we observed that, upon introduction of the magnetically functionalized microtubules into the flow cell, their orientation and transport in solution could be manipulated with a small permanent magnet. The fluorescence microscopy images in Figure 2 were obtained while the magnetic field orientation was

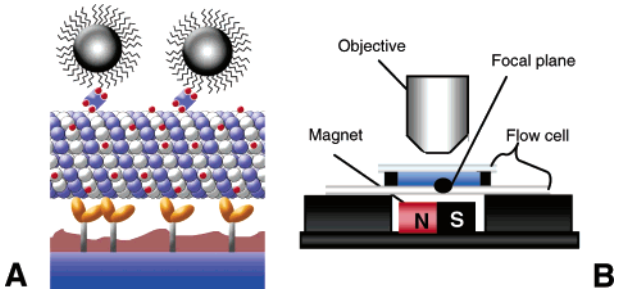

Figure 1. (A) Schematic of the microtubules functionalized with the cobalt ferrite particles on a kinesin surface. (B) Schematic of the magnet, flow cell, and objective configuration.

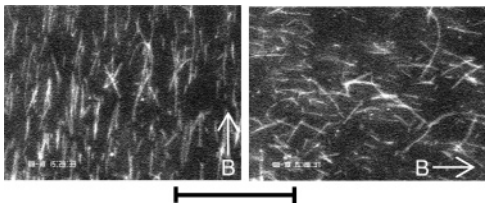

Figure 2. The orientation of magnetic microtubules as the field changes; time between each image is 4 s. Scale bar = 58 mm.

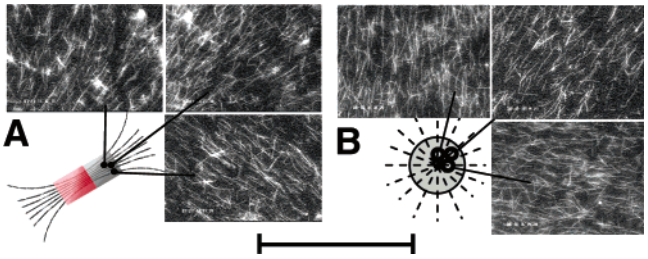

Figure 3. Fluorescence microscopy images of 37% biotinylated microtubules aligned with (A) a bar magnet for 3 min and (B) a cone magnet for 10 min. Scale bar = 116 μm. Also shown are the relative geometries of the magnets and magnetic field lines.

[†] Department of Chemistry.
[‡] Department of Bioengineering.

10.1021/ja055815s CCC: $30.25

Table 1. Gliding Speeds of Microtubules with Magnetic Cargo under Different Loading Conditions

	Surface Coverage (microtubules/10^4 μm^2)		Speed (μm/s)			
% biotin	no magnet	magnetically loaded	unmodified[c]	with neutravidin[d]	with $CoFe_2O_4$ particles[e]	magnetically aligned[f]
0	10 ± 3[b]		0.89 ± 0.05 (14)[g]			
37	6.9 ± 2.6[a]	133 ± 25[a]	0.87 ± 0.07 (16)[g]	0.29 ± 0.05 (48)[g]	0.25 ± 0.044 (61)[g]	0.22 ± 0.056 (59)[g]
85	0.62 ± 0.40[b]	140 ± 38[b]	0.88 ± 0.04 (17)[g]	0.024 ± 0.017 (50)[h]	0.024 ± 0.011 (52)[h]	0.005 ± 0.004 (38)[h]

[a] Density of microtubules after 10 min deposition time. [b] Density of microtubules after 3 min deposition time. [c] Average velocity of microtubules. [d] Microtubules with conjugated neutravidin. [e] Microtubules with neutravidin-conjugated $CoFe_2O_4$ particles, in absence of magnetic field. [f] Magnetically labeled microtubules loaded on a kinesin-modified surface. Values in parentheses represent the number of observed microtubules per analysis. [g] Less than 2% of observed microtubules are immobile. [h] Greater than 8% of observed microtubules are immobile.

altered by rotation of a cube-shaped magnet beneath the glass slide. The delay between images in Figure 2A and B is 4 s, within which time the majority of the microtubules have reoriented themselves to match the field lines. Relative to the small microtubules, larger rods rotate more slowly as the field direction is changed.

These data led us to hypothesize that magnetic fields could be utilized to orient microtubule arrays on the glass surface. The images shown in Figure 3 were obtained using magnets with two different geometries (cube and cone, Supporting Information) from various locations relative to the position of the magnet. The number of $CoFe_2O_4$-tagged microtubules that bind to the kinesin-modified surface under the influence of a magnetic field is significantly higher than that in the absence of a magnet or typically observed in standard motility assays (Table 1). Modification of the microtubules with magnetic nanoparticles somewhat decreases their ability to bind to the kinesin surface; however, the applied magnetic field significantly increases the surface concentration over an identical (or shorter) time period. In addition, the resulting microtubule surface density is strongly dependent on the distance from the magnet. For example, on top of the cube magnet, the microtubule surface coverage was 133 ± 25 /10^4 μm^2 (Figure 3A), whereas at a distance of 600 μm from the magnet the surface coverage dropped to 18 ± 5 /10^4 μm^2. These differences are expected based on the exponential decay of the magnetic field as a function of distance from the magnet and show that magnetic attractive forces pull the microtubules to the surface. While previous reports have demonstrated an enhanced microtubule surface density by application of an electric field,[10] the use of magnetically labeled microtubules and an external magnetic field rapidly loads the surface to similar surface densities but does not require microfabrication of embedded electrodes within the cell.

More importantly, magnetic loading creates ordered microtubule ensembles over large areas on the glass surface. In each case, the images in Figure 3 indicate alignment of the microtubules with an orientation that changes relative to the magnet. No such alignment was observed in the absence of an applied magnetic field or when biotin-labeled microtubules without magnetic nanoparticles were utilized. In experiments containing biotinylated microtubules and $CoFe_2O_4$ particles in the absence of neutravidin (i.e., the particles are not bound), no microtubule alignment was observed, demonstrating that the flow of free magnetic material in the solution does not cause the microtubules to align. Examination of the alignment patterns in Figure 3 reveals that the microtubules preferentially assemble with long-scale lateral order along the magnetic field lines (see Supporting Information). Alignment was consistent over the entire area of the magnet; to quantitatively assess its uniformity, the relative angle of orientation of the long axis of the microtubules was measured for 113 microtubules contained within a 4×10^3 μm^2 area. For these microtubules, the standard deviation of the orientation was found to be $\pm 19°$, comparable to previous reports of $\pm 10\%$ using alternative solution-flow methods,[5] yet in a more easily adjustable and controllable fashion.

Since other microtubule modifications have resulted in reduced transport velocities,[11] we next sought to test the gliding speed of the magnetically aligned microtubules over kinesin-functionalized surfaces in 1 mM ATP. A series of motility assays were performed with microtubules containing varying amounts of BTU (a) alone, (b) with bound neutravidin, and (c) with neutravidin-conjugated magnetic nanoparticles. Table 1 compares the motility of these microtubules to that of magnetically labeled microtubules that were loaded (and aligned) on the surface by application of the magnetic field prior to the addition of ATP. The microtubule gliding speeds depended strongly on both the presence and quantity of attached cargo. We find that the measured decrease in velocity is initiated by conjugation with neutravidin, and not by the nanoparticles per se. On the basis of this observation, we infer that the relatively large dimensions (80 nm^3) of this protein[12] inhibit kinesin−microtubule binding. While the 85% loaded microtubules showed the best alignment, the 37% BTU microtubules also have sufficient magnetic material to align and retain significant transport velocity both before and after application of a magnetic field. Future utility of this approach to create ordered microtubule ensembles will rely on optimization of the biotinylation and kinesin surface loading, or the magnetic particle attachment chemistry, to maximize both motility and control over transport of cargo.

Acknowledgment. This work was supported by a CAREER award from the National Science Foundation (to M.E.W., CHE0239-702) and by the Penn State Center for Nanoscale Science (MRSEC DMR0213623).

Supporting Information Available: Full experimental details, electron microscopy image of particles, and a wide-view fluorescence microscopy image of the magnetically patterned microtubules. This material is available free of charge via the Internet at http://pubs.acs.org.

References

(1) Goldstein, L. S. B.; Yang, Z. *Annu. Rev. Neurosci.* **2000**, *23*, 39.
(2) Bohm. K. J.; Stracke. R.; Muhlig. P.; Unger. E. *Nanotechnology* **2001**, *12*, 238.
(3) Yajima, J.; Alsonso, M. C.; Cross, R. A.; Toyoshima, Y. Y. *Curr. Biol.* **2002**, *12*, 301.
(4) Moorjani, S. G.; Jia, L.; Jackson, T. N.; Hancock, W. O. *Nano Lett.* **2003**, *3*, 633.
(5) (a) Brown, T. B.; Hancock, W. O. *Nano Lett.* **2002**, *2*, 1131. (b) Prots, I.; Stracke, R.; Unger, E.; Bohm, K. *J. Cell. Biol. Int.* **2003**, *27*, 251.
(6) (a) Glade, G.; Tabony, J. *Biophys. Chem.* **2005**, *115*, 29. (b) Vassilev, M. P.; Dronize, R. T.; Vassileva, M. P.; Georgiev, G. A. *Biosci. Rep.* **1998**, *2*, 1025.
(7) Sun, S.; Zeng, H.; Robinson, D. B.; Raoux, S.; Rice. P. M.; Wang, S. X.; Li, G. *J. Am. Chem. Soc.* **2004**, *126*, 273.
(8) Dubertret, B.; Skourides, P.; Norris, D. J.; Noireaux, V.; Brivanlou, A. H.; Libchaber, A. H. *Science* **2002**, *298*, 1759.
(9) Coy, D. L.; Wagenbach, M.; Howard, J. *J. Biol. Chem.* **1999**, *274*, 3667.
(10) Van den Heuvel, M. G. L.; Butcher, C. T.; Lemay, S. G.; Diez, S.; Cees, D. *Nano Lett.* **2005**, *5*, 235.
(11) Bachand, M.; Trent, A. M.; Bunker, B. C.; Bachand, G. D. *J. Nanosci. Nanotechnol.* **2005**, *5*, 718.
(12) Vermette, P.; Gengenbach, T.; Divisekera, U.; Kambouris, P. A.; Griesser, H. J.; Meagher, L. *J. Colloid Interface Sci.* **2003**, *259*, 13.

JA055815S